Science Journal of Chemistry
2015; 3(6): 84-90
Published online October 15, 2015 (http://www.sciencepublishinggroup.com/j/sjc)
doi: 10.11648/j.sjc.20150306.11
ISSN: 2330-0981 (Print); ISSN: 2330-099X (Online)

Physical, Thermal and Spectroscopic Studies of Biofield Treated *p*-Chlorobenzonitrile

Mahendra Kumar Trivedi[1], Alice Branton[1], Dahryn Trivedi[1], Gopal Nayak[1], Ragini Singh[2], Snehasis Jana[2, *]

[1]Trivedi Global Inc., Henderson, USA
[2]Trivedi Science Research Laboratory Pvt. Ltd., Hall-A, Chinar Mega Mall, Chinar Fortune City, Hoshangabad Rd., Bhopal, Madhya Pradesh, India

Email address:
publication@trivedisrl.com (S. Jana)

To cite this article:
Mahendra Kumar Trivedi, Alice Branton, Dahryn Trivedi, Gopal Nayak, Ragini Singh, Snehasis Jana. Physical, Thermal and Spectroscopic Studies of Biofield Treated *p*-chlorobenzonitrile. *Science Journal of Chemistry*. Vol. 3, No. 6, 2015, pp. 84-90.
doi: 10.11648/j.sjc.20150306.11

Abstract: Para-chlorobenzonitrile (*p*-CBN) is widely used as a chemical intermediate in the manufacturing of dyes, medicines, and pesticides, however; sometimes it may cause runaway reactions at high temperatures. The current study was designed to evaluate the impact of biofield energy treatment on the physical, thermal, and spectroscopic properties of *p*-CBN. The analysis was done by dividing the *p*-CBN samples into two groups that served as control and treated. The treated group received Mr. Trivedi's biofield treatment. Subsequently, the control and treated samples were evaluated using various analytical techniques such as X-ray diffraction (XRD), surface area analyser, differential scanning calorimetry (DSC), thermogravimetric analysis (TGA), Fourier-transform infrared (FT-IR) and UV-visible (UV-Vis) spectroscopy. The XRD results showed an increase in the crystallite size (66.18 nm) of the treated sample as compared to the control sample (53.63 nm). The surface area analysis of the treated sample also showed 14.19% decrease in the surface area as compared to control. Furthermore, DSC analysis results showed that the latent heat of fusion of the treated *p*-CBN increased considerably by 5.94% as compared to control. However, the melting temperature of the treated sample did not show any considerable change from the control sample. Besides, TGA/DTG studies showed that T_{max} (the temperature at which the sample lost its maximum weight) was increased by 5.22% along with an increase in its onset of thermal decomposition temperature *i.e.* 96.80°C in the biofield treated *p*-CBN as compared to the control sample (84.65°C). This indicates that the thermal stability of treated *p*-CBN sample might increase as compared to the control sample. However, no change was found in the FT-IR and UV-Vis spectroscopic character of the treated *p*-CBN as compared to the control. These findings suggest that the biofield treatment significantly altered the physical and thermal properties of *p*-CBN, which could make it more useful as a chemical intermediate.

Keywords: Biofield Energy Treatment, Para-Chlorobenzonitrile, X-ray Diffraction Study, Surface Area Analyzer, Differential Scanning Calorimetry, Thermogravimetric Analysis

1. Introduction

Aromatic nitriles have wide applications in the production of dyes, pesticides and pharmaceuticals. They are used as intermediates in the synthesis of various pharmacologically active compounds which are used as sedatives, muscle relaxants, neuroleptics, *etc*. [1]. They are also widely used in the synthesis of HIV-1 non-nucleoside reverse transcriptase inhibitors and the arylation of oxazoles and poly ether amides [2-4]. Benzonitriles are of great interest in the field of organic chemistry for the synthesis of pharmaceuticals, natural products, herbicides, and agrochemicals. Substituted benzonitriles are also used in the synthesis of various drugs like chlorazepate, climazolam and loflazepate, *etc.* [5]. Many derivatives of benzonitrile are used in salt form as urinary antiseptics and in vapour form for disinfecting bronchial tubes. *p*-Chlorobenzonitrile (*p*-CBN) is also used for N-arylation on benzimidazoles [6].

The stability profile of any chemical compound is the most desired quality that determines its shelf life and purity to be

used as an intermediate. The stability can be correlated to the physical, thermal or structural and bonding properties of a compound [7]. Currently, the stability of chemical compounds in pharmaceutical industries can be affected due to altering temperatures and pH conditions [8]. Moreover, many reactions in industries were carried out at high temperatures. Hence, the thermal stability is critical to ensure the safe handling of chemical compounds. The thermal stability is also considered in the processing, long-term storage or shipping of material. When a chemical has high stability, it is more resistant to breaking down or decomposition. The higher stability also helps to avoid runaway reactions [9]. However, benzonitriles are reported to cause runaway reactions during chlorination and cyanation reactions [10, 11]. Thus, it is important to search for an alternate strategy that can improve the stability of chemical compounds by altering their physical, thermal or structural and bonding properties.

In recent years, biofield energy has been known for its impact on various living organisms and non-living materials. A biofield is the electromagnetic field that permeates and surrounds living organisms, and the energy associated with this field is known as biofield energy [12, 13]. According to existing theories, this biofield constitutes a dynamic living matrix of information, which is responsible for communicating information to and throughout the body. It is believed that any imbalance in this biofield energy leads to disease. The health of living organisms can be affected by balancing this energy from the environment through a natural exchange process [14, 15]. Biofield therapies are very popular in holistic medicine health care systems, and are included in the National Centre for Complementary and Alternative Medicine (NCCAM), which is part of the National Institute of Health (NIH). NCCAM places biofield therapy (putative energy fields) as the subcategory of energy medicine among complementary and alternative medicines. [16, 17]. These healing treatments suggest their mechanism upon modulating patient-environmental energy fields. Thus, the human has the ability to harness the energy from the environment or universe and can transmit it to any living organism or non-living object. This process is termed as biofield treatment. Mr. Trivedi is well-known to possess a unique biofield energy treatment (The Trivedi Effect®) that has been significantly studied in different fields such as microbiology research [18-20], agriculture research [21,22], and biotechnology research [23,24]. Recently, it was reported that biofield treatment has changed the atomic, crystalline and powder characteristics as well as spectroscopic characters of different materials [25, 26]. Moreover, alteration in physical, thermal and chemical properties were also reported in materials like aluminium and ceramic oxide [27, 28]. Hence, based on above results the current study was designed to determine the impact of biofield treatment on physical, thermal and spectral properties of *p*-CBN.

2. Materials and Methods

p-chlorobenzonitrile (*p*-CBN) was procured from S D Fine Chemicals Pvt. Ltd., India. The sample was divided into two parts; one was kept as the control while other was subjected to biofield treatment and coded as treated sample. The control and treated samples were further characterizations using XRD, surface area analyser, DSC, TGA, FT-IR and UV-Vis spectroscopic techniques.

2.1. Biofield Treatment Modalities

p-chlorobenzonitrile was taken in this experiment for evaluating the impact of biofield treatment. The first set of the sample was considered as control, and no treatment was given to this part. The second set of the sample was handed over to Mr. Trivedi for biofield energy treatment under standard laboratory conditions. Mr. Trivedi provided the biofield treatment through his energy transmission process, which includes bioenergy emission for 3-5 min. without touching the sample. After treatment, the sample was handed over in the same condition and stored at standard conditions as per the standard experimental protocol. The optimum precautionary measures were taken while evaluating the physical, thermal, and spectra analysis throughout the experiments. The differences in parameters before and after the treatment were noted and compared.

2.2. X-ray Diffraction (XRD) Study

XRD analysis was carried out on Phillips, Holland PW 1710 X-ray diffractometer system. The X-ray generator was equipped with a copper anode with nickel filter operating at 35kV and 20mA. The wavelength of radiation used by the XRD system was 1.54056 Å. The XRD spectra were acquired over the 2θ range of 10°-99.99° at 0.02° interval with a measurement time of 0.5 seconds per 2θ intervals. The data obtained were in the form of a chart of 2θ *vs.* intensity and a detailed table containing peak intensity counts, d value (Å), peak width (θ°), and relative intensity (%).

The average size of crystallite (G) was calculated from the Scherrer equation (1) with the method based on the width of the diffraction patterns obtained in the X-ray reflected crystalline region.

$$G = k\lambda/(bCos\theta) \quad (1)$$

Where, k is the equipment constant (0.94), λ is the X-ray wavelength (0.154 nm), B in radians is the full-width at half of the peaks and θ the corresponding Bragg angle.

Percent change in crystallite size was calculated using the following equation (2):

$$\text{Percent change in crystallite size} = [(G_t-G_c)/G_c] \times 100 \quad (2)$$

Where, G_c and G_t are crystallite size of control and treated powder samples respectively.

2.3. Surface Area Analysis

The surface area was measured by the Surface area analyser, Smart SORB 90 based on Brunauer–Emmett–Teller (BET). Percent changes in surface area were calculated using

following equation (3):

$$\% \text{ change in surface area } = \frac{[S_{\text{Treated}} - S_{\text{Control}}]}{S_{\text{Control}}} \times 100 \quad (3)$$

Where, S_{Control} and S_{Treated} are the surface area of control and treated samples, respectively.

2.4. Differential Scanning Calorimetry (DSC) Study

Differential scanning calorimeter (DSC) of Perkin Elmer/Pyris-1 was used for studies related to melting temperature and latent heat of fusion (ΔH). The DSC curves were recorded under air atmosphere (5 mL/min) and a heating rate of 10°C/min in the temperature range of 50°C to 350°C. An empty pan sealed with cover pan was used as a reference sample. Melting temperature and latent heat of fusion were obtained from the DSC curve.

Percent change in latent heat of fusion was calculated using following equations (4) to observe the difference in thermal properties of treated *p*-CBN sample as compared to control:

$$\% \text{ change in latent heat of fusion } = \frac{[\Delta H_{\text{Treated}} - \Delta H_{\text{Control}}]}{\Delta H_{\text{Control}}} \times 100 \quad (4)$$

Where, $\Delta H_{\text{Control}}$ and $\Delta H_{\text{Treated}}$ are the latent heat of fusion of control and treated samples, respectively.

2.5. Thermogravimetric Analysis/ Derivative Thermogravimetry (TGA/DTG)

Thermal stability of control and treated sample of *p*-CBN was analysed using Mettler Toledo simultaneous thermogravimetric analyser (TGA/DTG). The samples were heated from room temperature to 400ºC with a heating rate of 5ºC/min under air atmosphere. From TGA curve, onset temperature T_{onset} (temperature at which sample start losing weight) and from DTG curve, T_{max} (temperature at which sample lost its maximum weight) were recorded.

Percent change in temperature at which maximum weight loss occur in sample was calculated using following equation (5):

$$\% \text{ change in } T_{max} = [(T_{max,\ treated} - T_{max,\ control}) / T_{max,\ control}] \times 100 \quad (5)$$

Where, $T_{max,\ control}$ and $T_{max,\ treated}$ are the temperature at which maximum weight loss occurs in control and treated sample, respectively.

Percent change in onset peak temperature was calculated using following equation (6):

$$\% \text{ change in onset peak temperature, } T_{onset} = [(T_{onset,\ treated} - T_{onset,\ control}) / T_{onset,\ control}] \times 100 \quad (6)$$

Where, $T_{onset,\ control}$ and $T_{onset,\ treated}$ are onset peak temperature in control and treated sample, respectively.

2.6. Fourier Transform-Infrared (FT-IR) Spectroscopic Characterization

The samples were crushed into fine powder for analysis. The powdered sample was mixed in spectroscopic grade KBr in an agate mortar and pressed into pellets with a hydraulic press. FT-IR spectra were recorded on Shimadzu's Fourier transform infrared spectrometer (Japan). FT-IR spectra are generated by the absorption of electromagnetic radiation in the frequency range 4000-400 cm^{-1}. The FT-IR spectroscopic analysis of *p*-CBN was carried out to evaluate the impact of biofield treatment at atomic and molecular level like bond strength, stability, rigidity of structure, *etc*. [29].

2.7. UV-Vis Spectroscopic Analysis

The UV-Vis spectral analysis was measured using Shimadzu UV-2400 PC series spectrophotometer over a wavelength range of 200-400 nm with 1 cm quartz cell and a slit width of 2.0 nm. This analysis was performed to evaluate the effect of biofield treatment on the structural property of *p*-CBN sample. With UV-Vis spectroscopy, it is possible to investigate electron transfers between orbitals or bands of atoms, ions and molecules existing in the gaseous, liquid and solid phase [29].

3. Results and Discussion

3.1. X-ray Diffraction

X-ray diffraction analysis was conducted to study the crystalline nature of the control and treated sample of *p*-CBN. XRD diffractogram of control and treated samples of *p*-CBN are shown in Figure 1. The XRD diffractogram of control *p*-CBN showed intense crystalline peaks at 2θ equal to 14.11°, 15.27°, 19.61°, 25.26° and 28.39°. The intense peaks indicated the crystalline nature of *p*-CBN. However, the XRD diffractogram of treated *p*-CBN showed the crystalline peak at 2θ equal to 14.05°, 15.27°, 19.55°, 25.16°, and 28.34°. Most of the treated sample peaks showed similar intensity as compared to the control that indicated that crystallinity of treated *p*-CBN sample was not changed as compared to control. Besides, the crystallite size was found as 53.63 and 66.18 nm in control and treated *p*-CBN, respectively. The crystallite size was increased by 23.4% in treated *p*-CBN as compared to control (Fig. 1). It was previously reported that cyano group has donor-acceptor interactions with electron-deficient groups like halogens thereby forming C≡N---halogen interactions. These interactions may lead to the formation of one or two dimensional network of molecules [30]. It is presumed that biofield energy may be absorbed by the treated *p*-CBN molecules that may lead to the formation of a supramolecular structure of *p*-CBN due to the interaction of C≡N---Cl. This formation of supramolecular structure may lead to increase in crystallite size of *p*-CBN after biofield treatment. This type of interaction was also reported by D. Britton in 2-chlorobenzonitriles, which lead to the formation of four crystallographic non-equivalent forms of molecules [31]. As the intermolecular bonding leads to stability of the compound, hence it suggests that biofield treatment might enhance the stability of treated *p*-CBN.

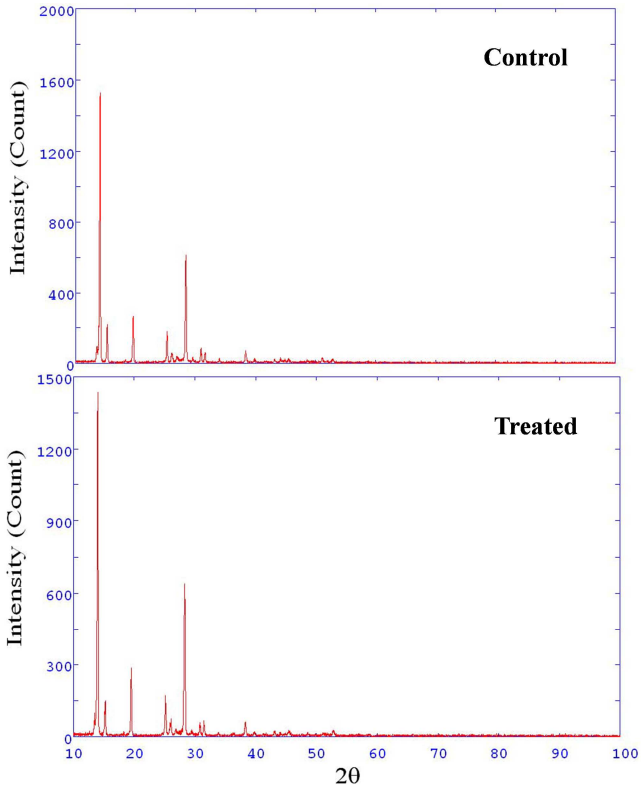

Fig. 1. X-ray diffractogram of control and treated samples of p-chlorobenzonitrile.

3.2. Surface Area Analysis

The surface area of control and treated samples of *p*-CBN was investigated using BET method. The control sample showed a surface area of 0.620 m^2/g; however, the treated sample of *p*-CBN showed a surface area of 0.532 m^2/g. The decrease in surface area was 14.21% in the treated *p*-CBN sample as compared to control (Fig. 2). As it was evident from XRD studies that after biofield treatment, the crystallite size of the *p*-CBN sample was increased, hence it could lead to decrease the surface area of treated sample as compared to control.

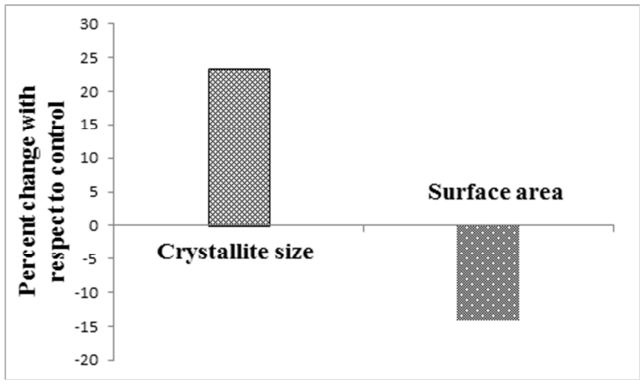

Fig. 2. Percent change in crystallite size and surface area of treated sample of p-chlorobenzonitrile as compared to control.

3.3. DSC Analysis

DSC was used to determine the latent heat of fusion (ΔH) and melting temperature in control and treated sample of *p*-CBN. The DSC analysis results of control and treated samples of *p*-CBN are presented in Table 1. The data showed that ΔH was increased from 113.15 J/g (control) to 119.88 J/g in treated *p*-CBN. It indicated that ΔH was increased by 5.95% in treated sample as compared to control (Fig. 3). It is presumed in XRD studies that biofield energy was absorbed by *p*-CBN molecules that possibly led to the formation of intermolecular bonding between chlorine-cyano groups in *p*-CBN molecules. Hence, the treated *p*-CBN sample needs more energy in the form of ΔH to undergo the process of melting. Previously, our group reported that biofield treatment has altered latent heat of fusion in lead and tin powder [27, 32]. Moreover, a slight change was observed in melting point of treated *p*-CBN (91.85°C) as compared to control sample (92.19°C).

3.4. TGA/DTG Analysis

Thermogravimetric analysis/derivative thermogravimetry analysis (TGA/DTG) of control and biofield treated samples are summarized in Table 1. The data showed that control *p*-CBN sample started losing weight at 84.65°C (onset) however; the treated *p*-CBN started losing weight at 96.80°C (onset). It indicated that onset temperature of treated *p*-CBN was increased by 14.35% as compared to control (Figure 3). Besides, the data showed T_{max} at 129.36°C in control, whereas, it was increased to 136.12°C in treated *p*-CBN (Table 1). It indicated that T_{max} was increased by 5.23% in treated *p*-CBN (Fig. 3). The increase in onset temperature can be related to increasing in thermal stability of treated *p*-CBN. As it was interpreted from DSC studies that ΔH was increased which may be due to the formation of intermolecular bonding between Cl---CN group after biofield treatment. Hence, this interaction might improve the stability of treated *p*-CBN sample at high temperature. The result was also evident by T_{max} value that was increased by 5.22% in treated sample; hence suggest that the temperature at which maximum weight loss occurred was increased in treated sample as compared to control.

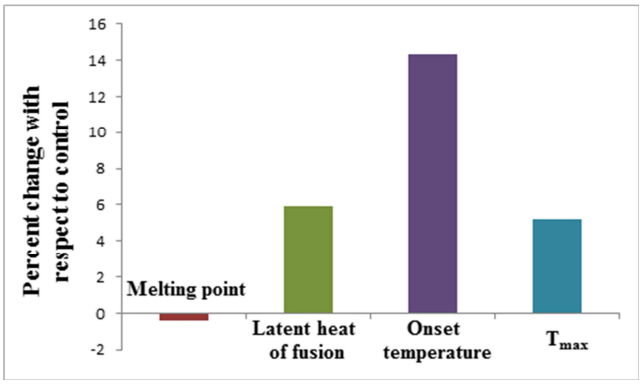

Fig. 3. Percent change in melting point, latent heat of fusion, onset temperature and T_{max} of treated sample of p-chlorobenzonitrile as compared to control.

Benzonitriles sometimes face the problem of runaway

reaction; hence thermal stability is critical to ensure their safe handling. From the thermal analysis data, it was presumed that treated *p*-CBN may be more thermally stable than control sample, and it might reduce the problems associated with it. The high stability also makes it more resistant to breaking down or decomposition. The thermal stability is also considered during processing, long-term storage or shipping of material [9].

Table 1. *Thermal analysis of control and treated samples of p-chlorobenzonitrile.*

Parameter	Control	Treated
Latent heat of fusion ΔH (J/g)	113.15	119.88
Melting point (ºC)	92.19	91.85
Onset temperature (ºC)	84.65	96.80
T_{max} (ºC)	129.36	136.12

T_{max}: temperature at which maximum weight loss occur

3.5. Spectroscopic Studies

3.5.1. FT-IR Analysis

The FT-IR spectra of control and treated samples are shown in Fig. 4. The spectra showed characteristic vibrational frequencies as follows:

Carbon - hydrogen vibrations

The aromatic structure of *p*-CBN showed the presence of C-H stretching vibrations in the region 3100-3000 cm^{-1} which was the characteristic region. The peaks of C-H stretching were observed at 3068 and 3091 cm^{-1} in both samples, *i.e.* control and treated. The C-H bending vibrations were observed at 1485, 1280, 1265 and 1170 cm^{-1} in the control sample. The peaks corresponding to C-H bending vibrations in treated sample were observed at 1487, 1280, 1261 and 1176 cm^{-1}.

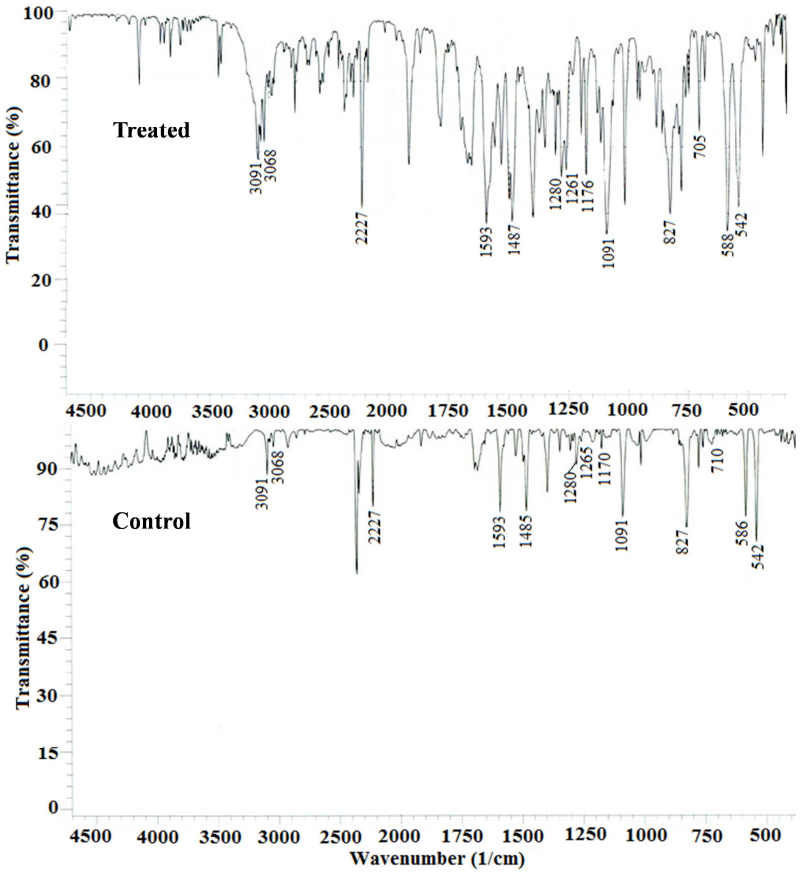

Fig. 4. *FT-IR spectra of control and treated samples of p-chlorobenzonitrile.*

Carbon- carbon vibrations

In the present study, the C-C stretching vibrations were observed at 1593 and 1091 cm^{-1} in the control sample. The treated sample also showed C-C stretching vibrations at same frequencies *i.e.* 1593 and 1091 cm^{-1}.

C-Cl vibrations

The vibrations belonging to the bond between the ring and halogen atoms may mix with other vibrations due to lowering of molecular symmetry and presence of heavy atoms on the periphery of the molecule. The C-Cl stretching vibrations generally give strong bands in the region of 710-505 cm^{-1}. In the control *p*-CBN sample, the peak at 586 cm^{-1} was assigned to C-Cl stretching. In treated sample, the peak due to C-Cl stretching was appeared at 588 cm^{-1}.

C≡N vibrations

For the aromatic compound that bears a C≡N group attached to the ring, a band of good intensity has been observed in the region of 2240-2221 cm^{-1} due to C≡N stretching [33]. In both control and treated samples, the peak due to C≡N stretching was observed at 2227 cm^{-1}. The C≡N in-plane bending vibrations were observed at 542 cm^{-1} in both control and treated samples of *p*-CBN.

Ring vibration

The peak due to disubstituted benzene was appeared at 827 cm^{-1} in both control and treated samples. Another peak due to ring breathing was appeared at 710 cm^{-1} in control sample whereas, at 705 cm^{-1} in treated sample.

The overall analysis was supported by literature data [33,34] and showed that there was no significant difference between observed frequencies of control and treated samples. Hence, it showed that biofield treatment might not induce any significant change at bonding level

3.5.2. UV-Vis Spectroscopic Analysis

The UV spectra of control and treated samples of *p*-CBN are shown in Fig. 5. The UV spectrum of control sample showed characteristic absorption peaks at 204 and 235 nm. The treated sample also showed absorption of light at the same wavelength. The peaks were appeared at 204 and 235 nm in treated sample of *p*-CBN. It suggests that biofield treatment may not cause any change in structure or position of the functional group as well as the energy which is responsible for electron transfers between orbitals or bands of atoms, ions and molecules.

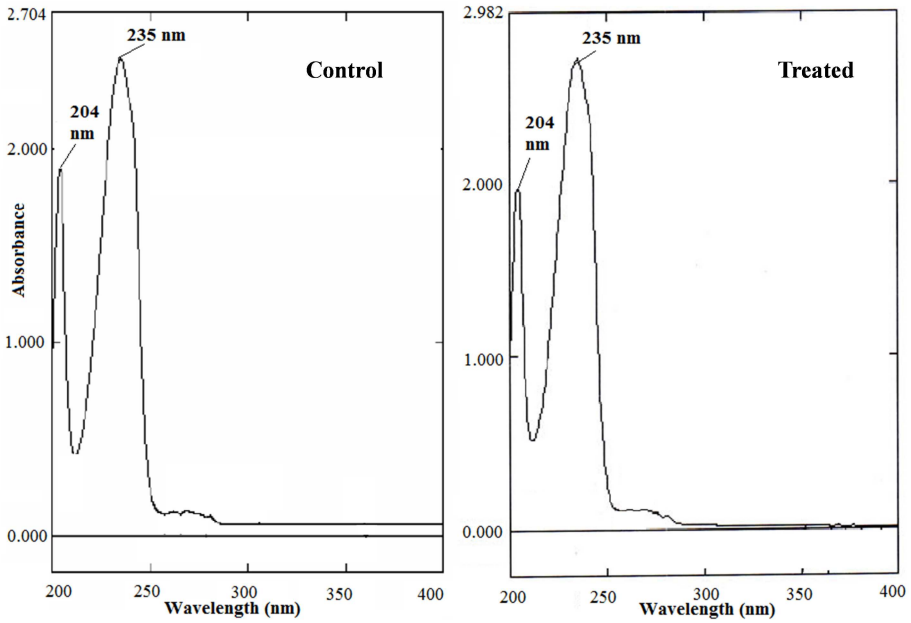

Fig. 5. *UV-Vis spectra of control and treated samples of p-chlorobenzonitrile.*

4. Conclusion

The XRD results showed that the crystallite size was increased by 23% in the treated *p*-CBN sample as compared to the control, which might be due to the formation of intermolecular bonding between CN and Cl groups of *p*-CBN. The surface area analysis showed a 14.19% decrease in the surface area of the treated *p*-CBN sample as compared to the control that which may be a result of increase in crystallite size of the *p*-CBN sample after the biofield treatment. DSC analysis data revealed that the latent heat of fusion was increased by 5.94% in treated the *p*-CBN as compared to the control. TGA/DTG studies showed that the onset temperature and T_{max} were increased by 14.35% and 5.22%, respectively, in the treated *p*-CBN sample. On the basis of thermal analysis data, it is hypothesized that the thermal stability of the treated *p*-CBN sample probably increased, which may affect its shelf life and efficacy along with safety when used in various chemical reactions. Therefore, it is assumed that the biofield treated *p*-CBN could be more useful and safe in the production of various pharmaceutical products.

Acknowledgments

The authors would like to acknowledge the whole team from the Sophisticated Analytical Instrument Facility (SAIF), Nagpur, Indian Rubber Manufacturers Research Association (IRMRA), Thane and MGV Pharmacy College, Nashik for providing the instrumental facility. We are very grateful for the support of Trivedi Science, Trivedi Master Wellness and Trivedi Testimonials in this research work.

References

[1] Fabiani ME (1999) Angiotensin receptor subtypes: Novel target for cardiovascular therapy. Drug News Perspect 12: 207-216.

[2] Tucker TJ, Sisko JT, Tynebor RM, Williams TM, Felock PJ, et al. (2008) Discovery of 3-{5-[(6-amino- 1H-pyrazolo[3,4-b]pyridine-3-yl)methoxy]-2- chlorophenoxy} - 5-chlorobenzonitrile (MK-4965): A potent, orally bioavailable HIV-1 non-nucleoside reverse transcriptase inhibitor with improved potency against key mutant viruses. J Med Chem 51: 6503-6511.

[3] Derridj F, Djebbar S, Benali-Baitich O, Doucet H (2008) Direct arylation of oxazole and benzoxazole with aryl of heteroaryl halides using palladium-diphosphine catalyst. J Organomet Chem 693: 135-144.

[4] Liu C, Zhang SH, Wang MJ, Liang QZ, Jian XG (2005) Synthesis and characterization of poly (ether amide)s containing bisphthalazinone and ether linkages. Chin Chem Lett 16: 437-439.

[5] Mahajan SS, Mahalakshmi A (2006) Synthesis of 2-amino-5-chlorobenzonitrile. Indian J Chem 45B: 1299-1300.

[6] Babu SG, Karvembu R (2011) CuO Nanoparticles: A simple, effective, ligand free, and reusable heterogeneous catalyst for N-arylation of benzimidazoles. Ind Eng Chem Res 50: 9594-9600.

[7] Blessy M, Patel RD, Prajapati PN, Agrawal YK (2014) Development of forced degradation and stability indicating studies of drugs-A review. J Pharm Anal 4: 159-165.

[8] Panyachariwat N, Steckel H (2014) Stability of urea in solution and pharmaceutical preparations. J Cosmet Sci 65: 187-195.

[9] Rowe S (2007) The importance of a robust assessment procedure in protecting against rapid overpressure hazards. I Chem Eng Symp Ser No. 153.

[10] Nolan PF, Barton JA (1987) Some lessons from thermal-runaway incidents. J Hazard Mater 14: 233-239.

[11] Gustin JL, Fines A (1996) Safety of chlorination reactions. I Chem Eng Symp Ser No. 141.

[12] Rivera-Ruiz M, Cajavilca C, Varon J (2008) Einthoven's string galvanometer: The first electrocardiograph. Tex Heart Inst J 35: 174-178.

[13] Rubik B (2002) The biofield hypothesis: Its biophysical basis and role in medicine. J Altern Complement Med 8: 703-717.

[14] Saad M, Medeiros RD (2012) Distant healing by the supposed vital energy- Scientific bases. Complementary Therapies for the Contemporary Healthcare. U.S.

[15] Rae A (2006) Quantum Physics: A beginner's guide. One world publications.

[16] Thomas AH (2012) Hidden in plain sight: The simple link between relativity and quantum mechanics. Swansea, UK.

[17] NIH, National Center for Complementary and Alternative Medicine. CAM Basics. Publication 347. [October 2, 2008]. Available at: http://nccam.nih.gov/health/whatiscam/

[18] Trivedi MK, Patil S, Shettigar H, Gangwar M, Jana S (2015) An effect of biofield treatment on multidrug-resistant *Burkholderia cepacia*: A multihost pathogen. J Trop Dis 3: 167.

[19] Trivedi MK, Patil S, Shettigar H, Gangwar M, Jana S (2015) Antimicrobial sensitivity pattern of *Pseudomonas fluorescens* after biofield treatment. J Infect Dis Ther 3: 222.

[20] Trivedi MK, Patil S, Shettigar H, Bairwa K, Jana S (2015) Phenotypic and biotypic characterization of *Klebsiella oxytoca*: An impact of biofield treatment. J Microb Biochem Technol 7: 203-206.

[21] Sances F, Flora E, Patil S, Spence A, Shinde V (2013) Impact of biofield treatment on ginseng and organic blueberry yield. Agrivita J Agric Sci 35: 22-29.

[22] Lenssen AW (2013) Biofield and fungicide seed treatment influences on soybean productivity, seed quality and weed community. Agricultural Journal 8: 138-143.

[23] Nayak G, Altekar N (2015) Effect of biofield treatment on plant growth and adaptation. J Environ Health Sci 1: 1-9.

[24] Patil SA, Nayak GB, Barve SS, Tembe RP, Khan RR (2012) Impact of biofield treatment on growth and anatomical characteristics of *Pogostemon cablin* (Benth.). Biotechnology 11: 154-162.

[25] Trivedi MK, Tallapragada RM, Branton A, Trivedi D, Nayak G, et al. (2015) Potential impact of bio field treatment on atomic and physical characteristics of magnesium. Vitam Miner 3: 129.

[26] Trivedi MK, Patil S, Shettigar H, Singh R, Jana S (2015) An impact of biofield treatment on spectroscopic characterization of pharmaceutical compounds. Mod Chem appl 3: 159.

[27] Trivedi MK, Patil S, Tallapragada RMR (2015) Effect of biofield treatment on the physical and thermal characteristics of aluminium powders. Ind Eng Manag 4: 151.

[28] Trivedi MK, Nayak G, Patil S, Tallapragada RM, Latiyal O (2015) Studies of the atomic and crystalline characteristics of ceramic oxide nano powders after bio field treatment. Ind Eng Manage 4: 161.

[29] Pavia DL, Lampman GM, Kriz GS (2001) Introduction to spectroscopy. (3rdedn), Thomson Learning, Singapore.

[30] http://shodhganga.inflibnet.ac.in:8080/jspui/bitstream/10603/25653/9/09_chapter%202.pdf

[31] Britton D (2007) *o*-Chloro- and *o*-bromobenzo-nitrile: Pseudosymmetry and pseudo-isostructural packing. Acta Crystallogr C 63: o14-o16.

[32] Trivedi MK, Patil S, Tallapragada RM (2013) Effect of biofield treatment on the physical and thermal characteristics of silicon, tin and lead powders. J Material Sci Eng 2: 125.

[33] Krishnan AR, Saleem H, Subashchandrabose S, Sundaraganesan N, Sebastain S (2011) Molecular structure, vibrational spectroscopic (FT-IR, FT-Raman), UV and NBO analysis of 2-chlorobenzonitrile by density functional method. Spectrochim Acta A Mol Biomol Spectrosc 78: 582-589.

[34] Sudha S, Sundaraganesan N, Kurt M, Cinar M, Karabacak M (2011) FT-IR and FT-Raman spectra, vibrational assignments, NBO analysis and DFT calculations of 2-amino-4-chlorobenzonitrile. J Mol Struct 985: 148-156.